

# **Rotary Friction Welding of Copper Rods by Utilizing Lathe Machine**

By

MOHAMMAD IQBAL BIN ABDUL AZIZ (11468)

Dissertation submitted in partial fulfillment of  
the requirements for the  
Bachelor of Engineering (Hons)  
(Mechanical Engineering)

SEPTEMBER 2012

Universiti Teknologi PETRONAS  
Bandar Seri Iskandar  
31750 Tronoh  
Perak Darul Ridzuan

# **CERTIFICATION OF APPROVAL**

## **Rotary Friction Welding of Copper Rods by Utilizing Lathe Machine**

By

Mohammad Iqbal Bin Abdul Aziz

A project dissertation submitted to the  
Mechanical Engineering Programme  
Universiti Teknologi PETRONAS  
in partial fulfilment of the requirement for the  
BACHELOR OF ENGINEERING (Hons)  
(MECHANICAL ENGINEERING)

Approved by,

---

DR TURNAD LENGGO GINTA

UNIVERSITI TEKNOLOGI PETRONAS

TRONOH, PERAK

September 2012

## **CERTIFICATION OF ORIGINALITY**

This is to certify that I am responsible for the work submitted in this project, that the original work is my own except as specified in the references and acknowledgements, and that the original work contained herein have not been undertaken or done by unspecified sources or persons.

---

MOHAMMAD IQBAL BIN ABDUL AZIZ

## **ABSTRACT**

Due to unavailability of rotary friction welding machine in Universiti Teknologi PETRONAS, a study to use conventional lathe machine for rotary friction welding of copper rods is done.

A setup of a conventional lathe machine with 7.5kW power of motor was used. Rotational speed was selected as 2000 rpm, since this speed was the maximum speed of the machine and can heat the copper rods to a high temperature.

The characteristics of microstructure and microhardness in rotary friction welding of copper rods by utilizing conventional lathe machine were examined. The microstructure test showed processed copper rod had smaller grain size compared to unprocessed copper rod due to recrystallization and recovery of microstructure. The hardness of processed copper was lower than that of the unprocessed copper due to annealing effect.

This conventional lathe machine failed to join the copper rods. The major problem was due to high amplitude of vibration because of length of the coppers themselves and length of tailstock quill, the part that connected to stationary chuck. However, all tests were able to heat the copper rods to high temperatures until red heat occurred. So, there is a possibility for this machine to perform rotary friction welding of copper rods.

## **ACKNOWLEDGEMENT**

Alhamdulillah, thanks to Allah SWT, God the Almighty for His planning and blessing upon me. A million of thanks to my helpful supervisor, Dr. Turnad Lenggo Ginta for his guidance, time, and knowledge in supervising my final year project. Although the result of this project is not as what as expected, but his kindness of solving problems occurring during the fabrication and machining stage had helped me a lot. To all the lab technicians and lab assistants who help me a lot during the fabrication and experimental stages of my project, I owe them something that I cannot pay, thank you so much. My gratitude is to my friends and my family, who gave me support and encouragement in my studies.

## **TABLE OF CONTENTS**

CERTIFICATION	ii
ABSTRACT	iv
ACKNOWLEDGEMENT	v
LIST OF FIGURES	viii
LIST OF TABLES	xi
CHAPTER 1 INTRODUCTION	1
1.1 Background of Study	1
1.2 Problem Statement	2
1.3 Objectives and Scope of Study	2
1.4 Relevancy of this Project	2
CHAPTER 2 LITERATURE REVIEW	3
2.1 Introduction to Welding	3
2.2 Friction Welding	5
2.3 Journal References	9
2.4 Copper	18
2.5 Conventional Lathe Machine	19
CHAPTER 3 METHODOLOGY	20
3.1 Introduction	20
3.2 Flow Chart	21
3.3 Procedures	22
3.4 Key Milestones (FYP 2 Gantt Chart)	41
3.5 Tools Used	42
CHAPTER 4 RESULTS AND DISCUSSION	43
4.1 Result of Rotary Friction Welding	43
4.2 Processed Copper Rods	45
4.3 Microstructure Test	47
4.4 Microhardness Test	50

CHAPTER 5 CONCLUSION AND RECOMMENDATIONS	52
REFERENCES	54

## LIST OF FIGURES

Figure 1.1: Rotary friction welding on process	1
Figure 2.1: Friction Welding Process	7
Figure 2.2: Lathe Machine	8
Figure 2.3: Microphotos of (a) copper, (b) aluminium (Sahin, 2009)	9
Figure 2.4: Interface region in joints of aluminium and copper. (Sahin, 2009)	10
Figure 2.5: Hardness results on horizontal distance at interface of joints of copper-aluminium. (Sahin, 2009)	10
Figure 2.6: The effect of friction pressure on the microstructure. (Kurt et al. 2011)	11
Figure 2.7: The microhardness distribution of materials. (Kurt et al. 2011)	12
Figure 2.8: Microphotographs of the welding zone. (Sahin et al. 1998)	13
Figure 2.9: Microhardness test results of copper and steel bar. (Sahin et al. 1998)	14
Figure 2.10: Microstructure results of titanium alloys (Avinash et al. 2007)	15
Figure 2.11: Vickers Hardness test results of titanium alloys (Avinash et al. 2007)	15
Figure 2.12: Phases of conventional friction welding process. (Alves et al. 2010)	16
Figure 2.13: HV microhardness versus distance bonding interface. (Alves et al. 2010)	17
Figure 2.14: Photomicrograph of the interface bonding between the AA1050 aluminum and AISI 304 stainless steel with an increase of 100 X.(Alves et al. 2010)	17
Figure 2.6: Excel XL-510 Heavy Duty Lathe Machine	19
Figure 3.1: Unprocessed copper	22
Figure 3.2: Copper rods were clamped to chucks; one to the spindle chuck and another to the stationary chuck.	23
Figure 3.3: Copper rods were brought together as close as possible.	23
Figure 3.4: Rotational speed was adjusted.	23

Figure 3.5: Clutch was pushed down.	24
Figure 3.6: Spindle chuck was rotating.	24
Figure 3.7: Clutch was pulled up.	24
Figure 3.8: Measuring temperatures for both copper rods by using an infrared thermometer.	25
Figure 3.9: 60mm copper rod.	25
Figure 3.10: Dimension of 10mm to be cut.	26
Figure 3.11: Desired size of copper piece prior to mounting for both microstructure and microhardness test.	26
Figure 3.12: EDM wire cutting machine, Mitsubishi FA10	26
Figure 3.13: Copper rod was clamped.	27
Figure 3.14: Copper rod was placed to origin position.	27
Figure 3.15: By using controller, wire was brought close to the copper rod.	28
Figure 3.16: The cutting tank was filled up with water.	28
Figure 3.17: Movement of the cutting was programmed by using computer numerical controlled (CNC) drawing plotter.	29
Figure 3.18: Wire was cutting the copper rods.	29
Figure 3.19: Copper rods that had been cut.	29
Figure 3.20: Phenolic powder, manufactured by Buehler.	30
Figure 3.21: Compression mounting equipment: Simplimet 1000 Auto Mounting Press, manufactured by Buehler.	31
Figure 3.22: Mounted copper.	31
Figure 3.23: Grinding papers: Microcut Silicon Carbide Grinding Paper, manufactured by Buehler.	32
Figure 3.24: Grinder: Metaserv 2000, manufactured by Buehler.	32
Figure 3.25: Grinding process.	33
Figure 3.26: Polishing liquid: MetaDi Fluid 40-6032, manufactured by Buehler.	34
Figure 3.27: MetaDi Diamond Paste (Grade = 3, Mesh = 8000)	34
Figure 3.28: Polishing paste on mounted copper.	34
Figure 3.29: Polishing process.	35
Figure 3.30: Aqueous Ferric Chloride etching solution.	36
Figure 3.31: Etching solution on mounted copper.	36
Figure 3.32: Mounted copper was washed by water.	37
Figure 3.33: Mounted copper was washed by ethanol.	37



## **LIST OF TABLES**

Table 3.1: FYP 2 Gantt Chart	41
Table 3.2: Thermal Properties of copper	42
Table 4.1: Result of rotary friction welding process	44
Table 4.2: Microharness result of unprocessed copper	50
Table 4.3: Microhardness result of processed copper	51

# Chapter 1

## INTRODUCTION

### 1.1 Background of Study

In world of joining materials, welding is the most famous process. Developed in 1940s, friction welding can be classified into three types: rotary, linear, and friction stir welding. Rotary friction welding is the most common form of friction welding and has become an industry standard for a number of process.

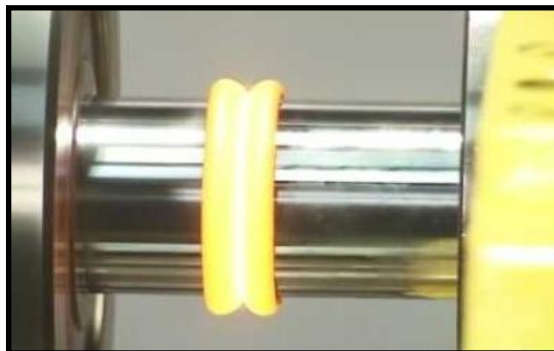


Figure 1.1: Rotary friction welding in progress.

By processing rotary friction welding, cross-sectional area are 100% welded. It requires no special weld interface preparation welding and no post machining is need for friction welded components in many cases. It is free from inclusion and gas porosity.

In manufacturing industry, high cost, multiple rotational speeds, and powerful machines are used to perform rotary friction welding. This study was carried out on whether rotary friction welding could be done by using a regular conventional lathes machine.

## **1.2 Problem Statement**

In manufacturing industry, the high cost, multiple rotational speeds, and powerful machines are used to perform rotary friction welding. Due to unavailability of rotary friction welding machine in Universiti Teknologi PETRONAS, the study to use conventional lathe machine for rotary friction welding of copper rods is necessary to be done. The welding temperature must be clearly investigated.

## **1.3 Objectives and Scope of Study**

The objectives of this project are:

1. To investigate the performance of lathe machine to do rotary friction welding.
2. To study the effect of spindle speed on microstructure and microharness.

This project will be run based on normal rotary friction welding process, but by using conventional lathe machine and applying axial pressure manually.

## **1.4 Relevancy of This Project**

By applying friction welding process, this project will focus on the problem whether a successful joint of copper rods can be created by using conventional lathes machine. Furthermore, investigation of temperature will be taken into consideration if the joint can be achieved. However, priority will be given to the successful joint fabrication.

## **CHAPTER 2**

### **LITERATURE REVIEW**

#### **2.1 Introduction to Welding**

##### **2.1.1 History**

Welding is not new. The earliest known form of welding, called forge welding, dates back to the year 2000 B.C. Forge welding is a primitive process of joining metals by heating and hammering until the metals are fused (mixed) together. Although forge welding still exists, it is mainly limited to the blacksmith.

There are many welding processes today. Welding is a process of permanent joining two materials (usually metals) through localized coalescence resulting from a suitable combination of temperature, pressure and metallurgical conditions. Depending upon the combination of temperature and pressure from a high temperature with no pressure to a high pressure with low temperature, a wide range of welding processes has been developed.

### 2.1.2 Types of Welding

Welding processes can be classified as follows (based on the source of energy):

- a) Gas Welding
  - Oxyacetylene
  - Oxy hydrogen
- b) Arc Welding
  - Carbon Arc
  - Metal Arc
  - Submerged Arc
  - Inert-gas-Welding  
TIG and MIG
  - Plasma Arc
  - Electro-slag
- c) Resistance Welding
  - Spot
  - Seam
  - Projection
  - Butt Welding
  - Induction Welding
- d) Solid State Welding
  - Friction Welding
  - Ultrasonic Welding
  - Explosive Welding
  - Forge and Diffusion Welding
- e) Thermo-chemical Welding
  - Thermit Welding
  - Atomic H<sub>2</sub> Welding
- f) Radiant Energy Welding
  - Electron Beam Welding
  - Laser Beam Welding

## **2.2 Friction Welding**

### **2.2.1 History**

Back to 1891, the first patent on the friction welding was issued in the USA, according to the American Welding Society. From 1920 to 1944, more patents were issued throughout Europe and in the USSR in 1956. In USA, further study of friction welding was developed by AMF (produced steering worm shaft welding machine), Caterpillar (produced turbochargers and hydraulic cylinders machines), and Rockwell International (built truck's spindle-housing welding machine).

In 1969, a linear reciprocating mechanism for welding mild steel patent was issued. In the early 1980s, viability of the LFW technique for metal using modified equipment was demonstrated by TWI. In the mid of 1980s, a prototype electro-mechanical machine with a linear reciprocating mechanism was designed and built. In 1991, TWI invented friction stir welding process.

The most extensive historical records are kept with the American Welding Society.

### **2.2.2 Types of Friction Welding**

In friction welding, the heat is required for welding is generated through friction at the interface of the two components being joined, like rubbing hands together rapidly.

#### Rotary

In this method, the energy required for frictional heating is supplied by the kinetic energy of a flywheel. The flywheel is accelerated to the proper speed, the two members are brought into contact, and an axial force is applied. The welds produced are excellent quality, featuring superior mechanical properties of the metals that were joined. This process can be used to fabricate suspension rods, steering columns, gear box forks and driveshaft's as well as engine valves.

#### Linear

This method is capable to join square or rectangular components (as well as round) made of metals or plastics. In this process, one part is moved across the face of the other part by a balanced reciprocating mechanism. It reduces raw material cost and improving quality with bi-material applications. The popular application is the fabrication or repair of integrated blades and disks.

#### Friction Stir

In this method, a third body is rubbed against the two surfaces to be joined. A rotating non-consumable probe is plunged into the joint, and forces mixing (or stirring) of the materials in the joint. This process is now being applied to aerospace, automotives, ship building, and military vehicles, using sheet or plates. Welds produced by friction stir welding have high quality, minimal pores, and a uniform material structure.

### 2.2.3 Rotary Friction Welding Process

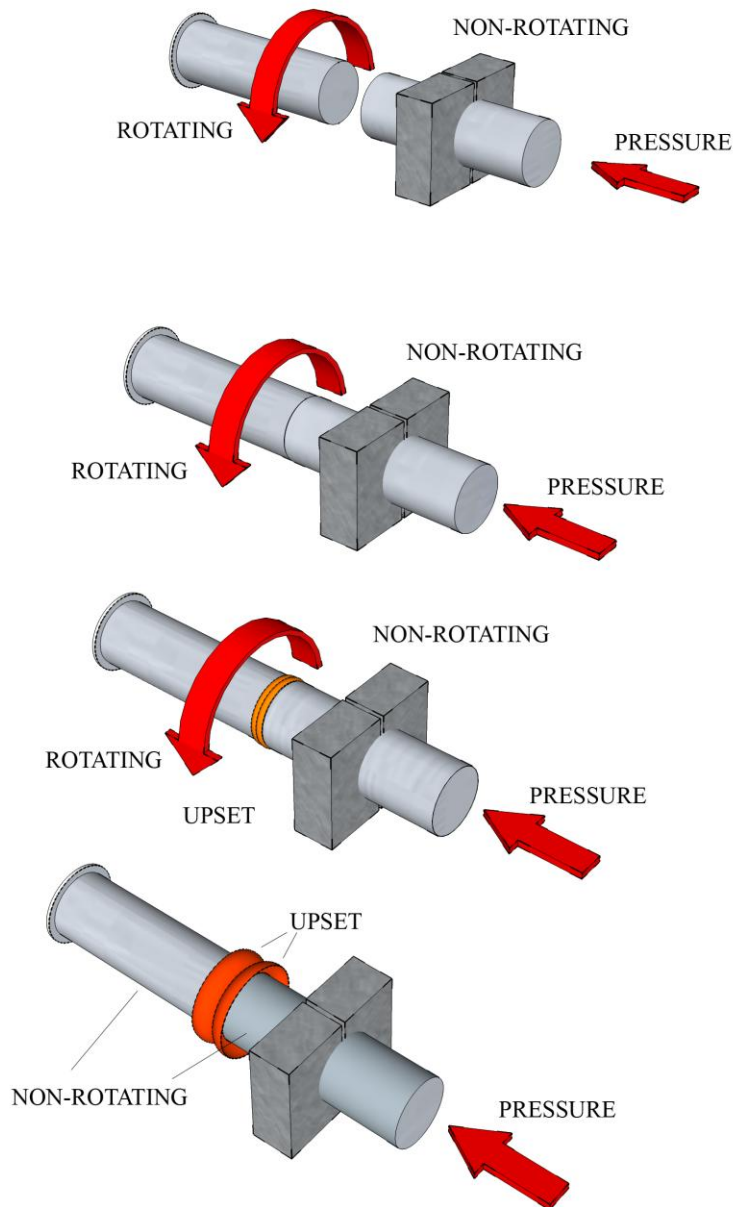


Figure 2.1: Friction Welding Process

In rotary friction welding, one of the components is clamped to a spindle chuck, usually attached to fly wheels, and the second component is held stationary to tailstock quill. The fly wheel and chuck assembly is rotated to a certain speed to store a predetermined amount of energy. Then, the drive to flywheel is declutched, and the two components are brought together under axial pressure ( $P_f$ ).

Friction between the parts decelerates the fly wheel converting stored energy into frictional heat. Then the drive is released and the rotary component is quickly stopped while the axial pressure is being increased to a higher predetermined upset pressure, for a predetermined time. Friction time, friction pressure, upset time, upset pressure and rotational speed are the parameters in this process of joining.

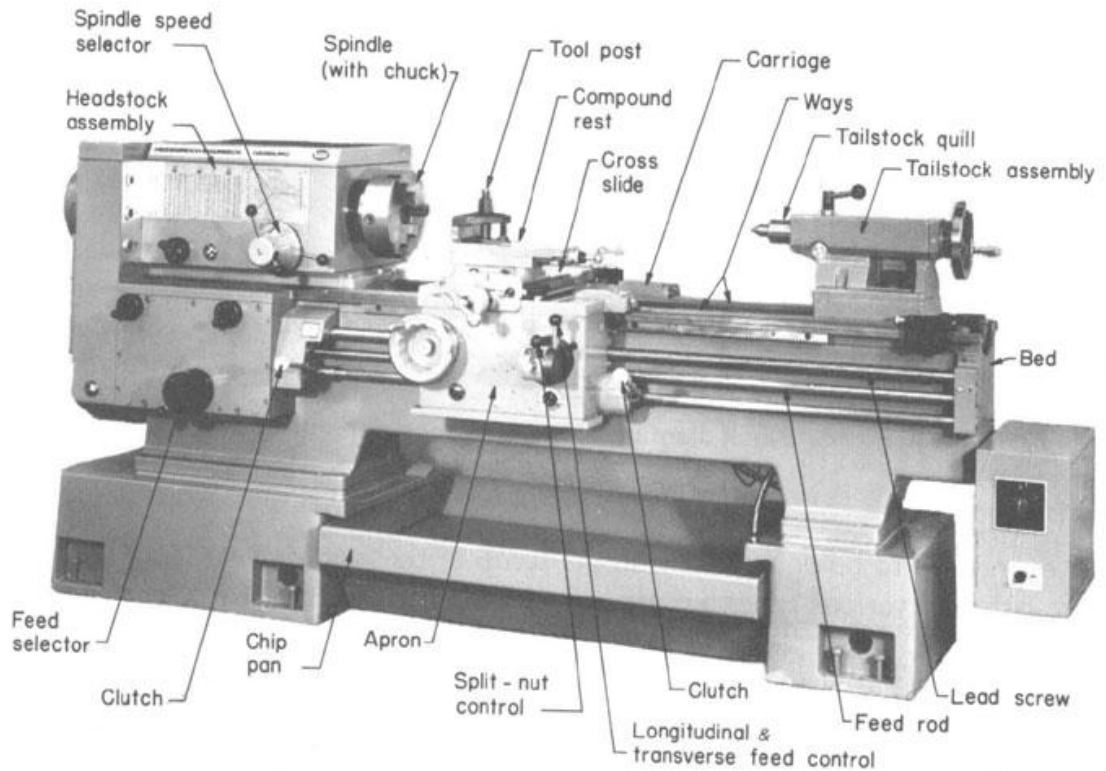
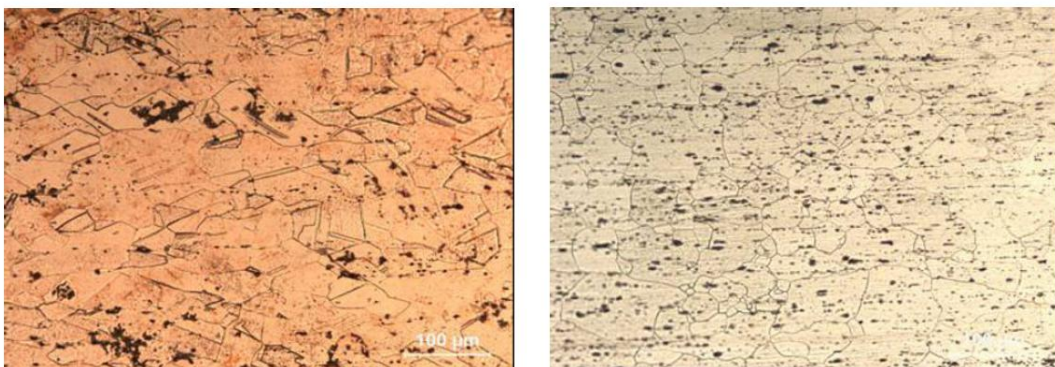


Figure 2.2: Lathe machine

### 2.3 Journal References

The author had decided to carry out some research on some previous rotary friction welding research through past journals. Below are the journals and the information that the author obtained from the journals.

Mumin Sahin (2009) studied the joining of copper and aluminum material with friction welding to get optimum parameters using a statistical approach. A setup of drive motor with 4 kW power and 1,410 rpm was selected as taking into account the friction and the upset pressures required for the torque capacity in friction welding of steel bars within 10 mm diameter. Friction and upset pressures can be observed on pressure indicator, and the stages of the welding sequence are controlled by solenoid valve driven by an external timer. Friction time, friction pressure and upset pressure have a direct effect on the tensile strength of joints. Linear statistical analysis was used in order to study the effect of these factors. Optimum parameters were found as; (60 MPa) for friction pressure, (120 MPa) for upset pressure and (2.5 s) for friction time. The minimum friction pressure in his study is 42 MPa, with a constant spindle speed of 1410 rpm.



(a)

(b)

Figure 2.3: Microphotos of (a) copper, (b) aluminium (Sahin, 2009)

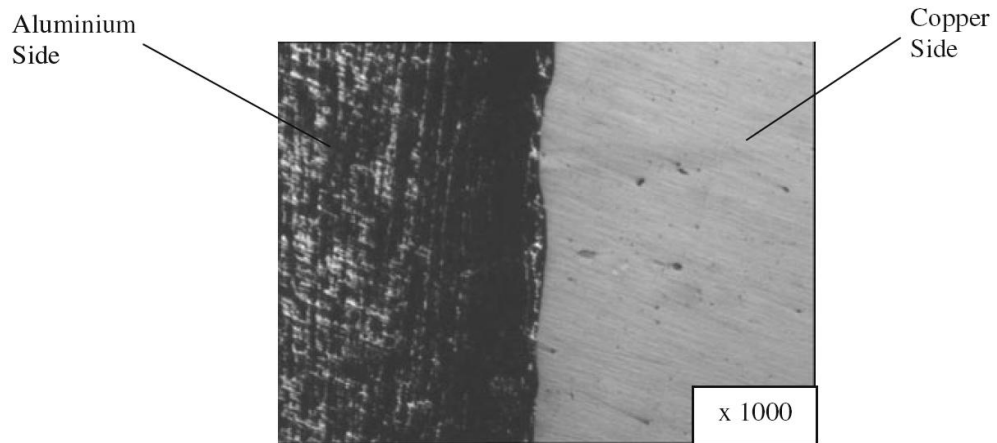


Figure 2.4: Interface region in joints of aluminium and copper. (Sahin, 2009)

Hardness variation was obtained under 200 g loads by Vickers microhardness testing (Figure 2.5). As the aluminium used in the present study was a cold drawn bar, it was already work hardened before friction welding. Aluminium recovered and recrystallised as a result of frictional heat and deformation, thus was slightly softened. Hardness variations on the copper side are more than those on the aluminium side. This variation is due to comparatively high thermal conductivity of copper.

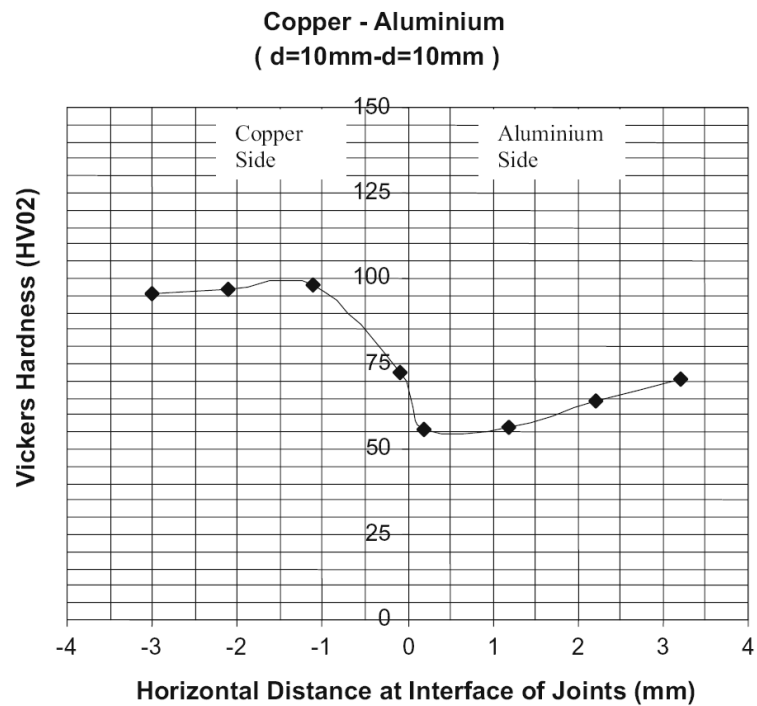


Figure 2.5: Hardness results on horizontal distance at interface of joints of copper-aluminium. (Sahin, 2009)

Kurt et al. (2011) investigated the influence of process parameters, which includes friction pressure, upset pressure, and upset time on the axial shortening, hardness, microstructure, and tensile properties of the welding of dissimilar AISI 1010 mild steel and ASTM B22 copper bronze. Cylindrical test specimens of 20 mm in diameter and 100 mm in length were prepared for friction welding. Joining of these two dissimilar alloys was performed on a continuous drive friction welding machine of 250 kN capacity at a constant rotation speed of 2500 rev/min, and constant friction time of 3 s. Friction and upset pressures can be observed on the screen, and the welding sequence stages are controlled by a solenoid valve. The welding parameters were as follows: friction pressures (P1): 10, 15, 20 MPa; upset pressures (P2): 22, 25, 30 MPa; and upset (forging) time (t1) of 1, 5, 7, 8 seconds. The minimum friction pressure was 10 MPa.

It is clearly seen that insufficient friction pressure on the joining surface resulted in an inadequate locking of the surfaces (Figure 2.6a) where limited plastic deformation and microstructural changes occurred, and these facts caused poor tensile response of the joint. An increase in the friction pressure caused better joining surfaces (Figure 2.6b and Figure 2.6c) where recrystallization occurs on the bronze side, and grain refinement and strain hardening occurs on the steel side. The width of the recrystallized region is mainly affected by the friction pressure. An increase in the friction pressure resulted in a wider fine grain region. A change in microstructure and axial shortening also notably occurred in the bronze side.

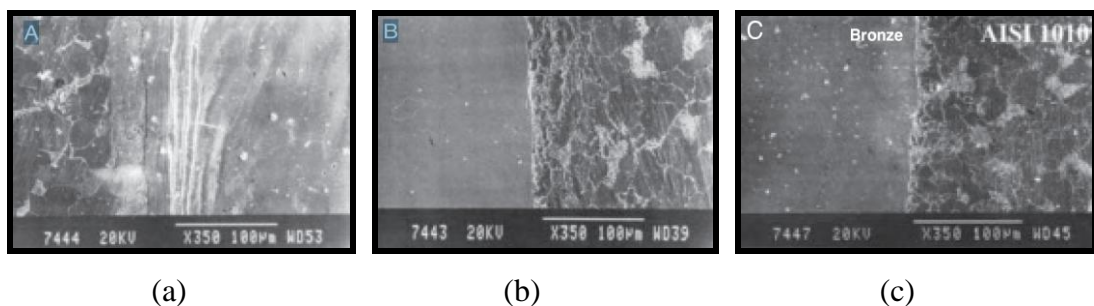


Figure 2.6: The effect of friction pressure on the microstructure. (a) P1 = 10 MPa, P2 = 22 MPa, t1 = 5 s. (b) P1 = 15 MPa, P2 = 22 MPa, t1 = 5 s. (c) P1 = 20 MPa, P2 = 22 MPa, t1 = 5 s. (Kurt et al. 2011)

Almost the same trend was observed in the microhardness profiles of all samples (Figure 2.7). The maximum hardness values of joints were obtained on the steel side next to the welding centerline. The hardness values generally increased with increasing friction pressure and upset pressures, but hardness values decreased with increasing upset time. Increasing hardness in the welding interface can be related to the microstructure formed in the weld interface as a result of the heat input and plastic deformation.

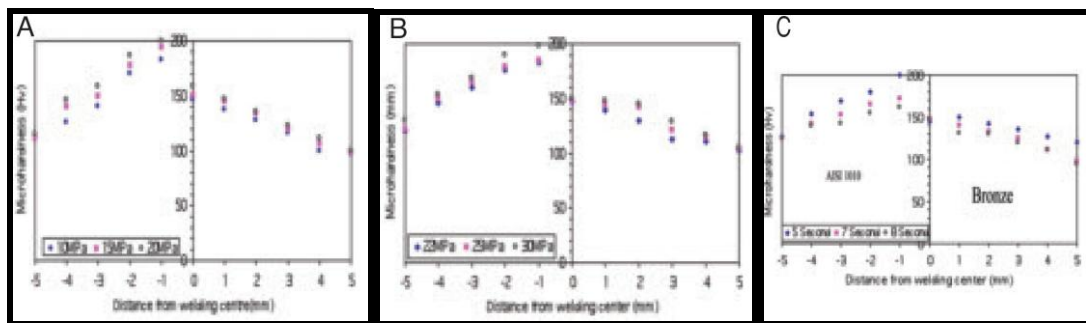


Figure 2.7: The microhardness distribution of materials. (a) The effect of friction pressure ( $P_2 = 22$  MPa,  $t_1 = 5$  s); (b) the effect of upset pressure ( $P_1 = 10$ , (b) MPa,  $t_1 = 5$ ); C — the effect of upset time ( $P_1 = 10$  MPa,  $P_2 = 30$  MPa). (Kurt et al. 2011)

Sahin, et al. (1998) did a statistical analysis for the affecting parameters on the mechanical properties of the resulting welding of copper and steel bars. The steel samples were H21 (DIN-X 30 W Cr V 93) and 1015 (DIN-1141) whilst the copper samples were 98%. Both of them were prepared as 10 mm diameter rods. The friction welder motor had operating capability up to 120 kN and had variable speed up to 3500 rpm. The speed, friction pressure, friction time, forging pressure, feed rate, brake delay time, upset delay time and upsetting time were controlled by a computer. The minimum spindle speed is 2000 rpm with applied load of 500 – 1274 kg.

The temperature developed in the outer region close to the free surface of the sample is higher than that corresponds to the central region of the sample, during welding process. This results in relatively large melting and heat-affected zones developing in this region. Small grains in the copper side indicate hardening, whilst no significant variation is observed in the grain size on the steel side (Figure 2.8).

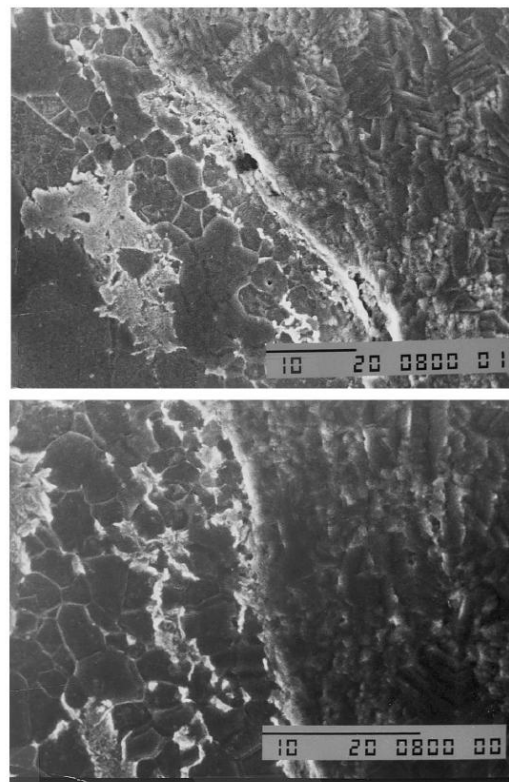


Figure 2.8: Microphotographs of the welding zone. (Sahin et al. 1998)

Around the interface, the hardness of the copper increases slightly. However, slight decrease in the hardness of the steel is observed (Figure 2.9). This is due to the steel reaching the annealing temperature during the welding process, which in turn reduces hardness on the steel side. On the other hand, copper exhibits hardening due to its high thermal conductivity and fast cooling behavior.

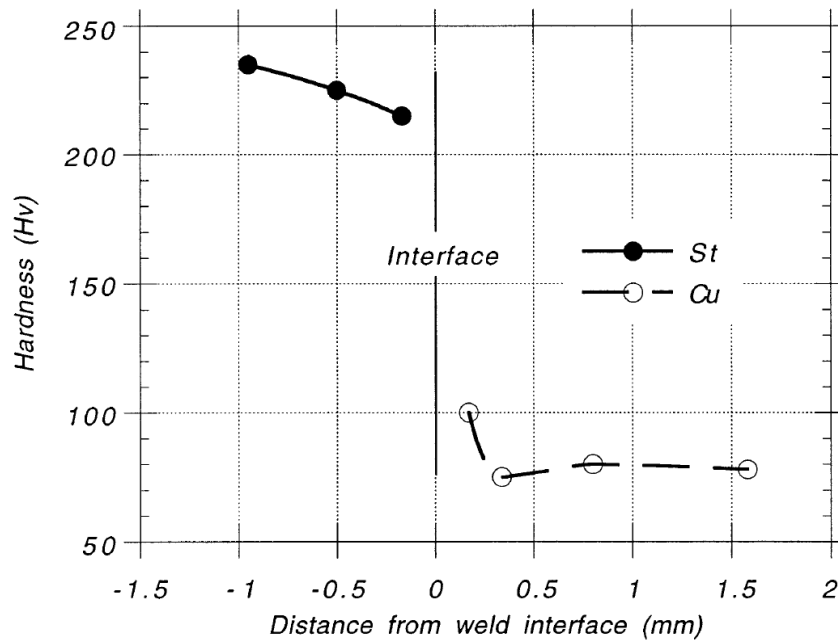


Figure 2.9: Microhardness test results of copper and steel bar. (Sahin et al. 1998)

Avinash et al. (2007) used titanium alloys, Ti-6Al-4V in their study. The titanium alloys contained 6% of Al, 3.92% of V, 0.2 max % of O, 0.25 max of Fe, and remaining of Ti. They were 100mm diameter rods. Rotational speeds of 1000rpm, 1500rpm and 2000rpm were used to produce the weld joints. The other parameters of the process are: soft force: 0.1 ton; upset force: 0.3 tons; friction force: 0.15 tons, upset time: 2 seconds and burn off: 4mm. These were kept constant.

There is a distinct deformed zone on either side of the weld interface. This is the Transition Zone (TZ). The effect of rotation of the specimen before welding can be seen in this zone, as the grains are pulled in the direction of rotation, being subjected to torque at high temperature. The degree of deformation appears to be very high. In the TZ of the weld, between the welded interface and the parent metal, very large grains are formed. This shows the effect of dynamic recrystallization. Increasing speed has made the grains have grown to be larger and there is a marked distinction between the structures of the two pieces welded (Figure: 2.10). The hardness value also increased (Figure: 2.11).

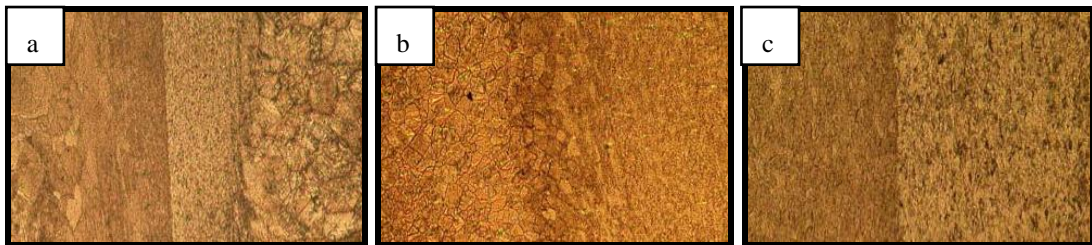
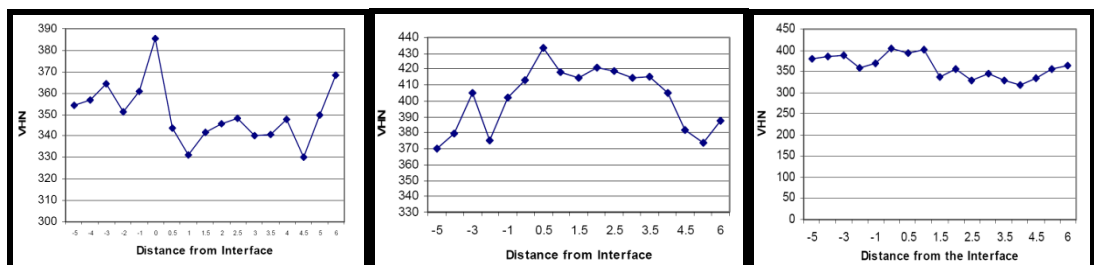


Figure 2.10: Microstructure results of titanium alloys (a) 1000rpm, (b) 1500rpm, (c) 2000rpm (Avinash et al. 2007)



(a)

(b)

(c)

Figure 2.11: Vickers Hardness test results of titanium alloys (a) 1000rpm, (b) 1500rpm, (c) 2000rpm (Avinash et al. 2007)

Alves et al. (2010) obtained junctions between the AA1050 aluminum (commercially pure aluminum, 99.5% Al) and AISI 304 stainless steel. After obtaining the best results (the fracture occurred away from the bonding interface) in the AA1050 aluminum (lower resistance), the process was optimized and analyzed in the bonding interface by optical microscopy, electron microscopy of EDX and Vickers microhardness test.

The main parameters used to perform the set up are: Pressure  $P_1$  and time  $t_1$  – heating phase; Pressure  $P_2$  and time  $t_2$ – forging phase; and rotation per minute (rpm). Figure 2.12 shows the phases of the process.

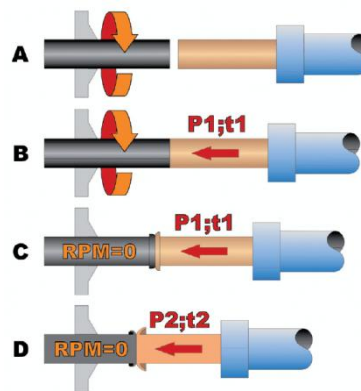


Figure 2.12: Phases of conventional friction welding process. (A) Period of approximation; (B)  $P_1, t_1$  application; (C) end of  $P_1, t_1$  application, and braking of the machine ( $RPM = 0$ ); (D)  $P_2, t_2$  application and finish welding. (Alves et al. 2010)

A rotary friction welding machine of brand GATWIK was used with fixed speed of 3,200 RPM,  $P_1 = 2.1$  MPa,  $t_1 = 32$  seconds,  $P_2 = 1.4$  MPa and  $t_2 = 2$  seconds.

A sample with the same parameters of the junction which showed 100% of efficiency was analyzed by Vickers microhardness using a digital microhardness tester (Future-Tech Corporation, Japan) with a 300 gF load (stainless steel) and 100 gF (aluminum) for 10 seconds. Microhardness was conducted at the interface of the weld and in the regions near both the aluminum and the AISI 304 stainless steel sides (Figure 2.13).

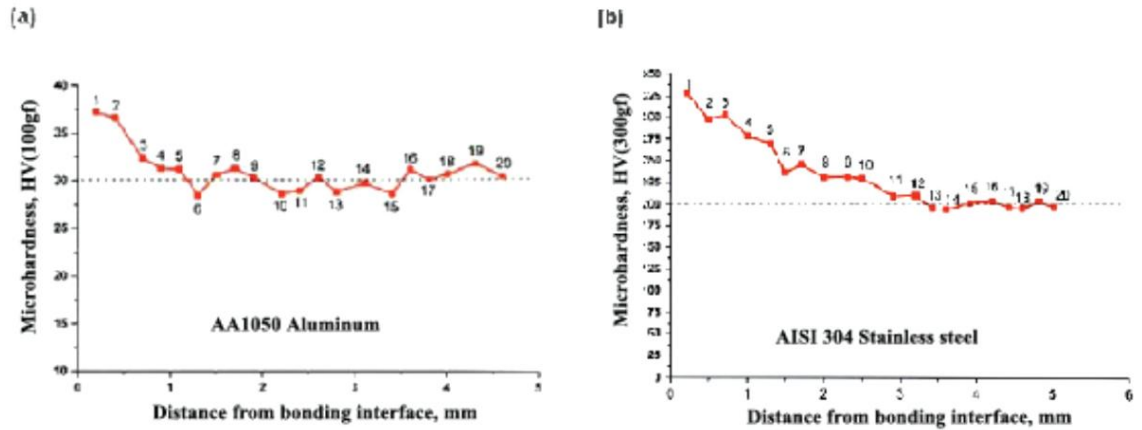


Figure 2.13: HV microhardness versus distance bonding interface. (a) AA1050 aluminum; (b) AISI 304 stainless steel. (Alves et al. 2010)

Microstructure test showed the interface region is characterized by a straight line with some imperfections under the friction welding process. Both in the aluminum and stainless steel sides, microstructural changes are not observed near the interface region, as it occurs in fusion welding processes (Figure 2.14). All plastic deformation resulting from the parameters used in the process occurred in the AA1050 aluminum, due to the fact that this material has lower strength and lower hot forging temperature.

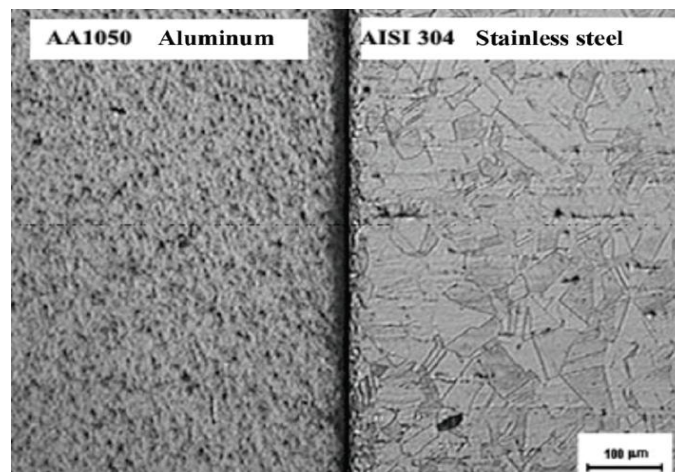


Figure 2.14: Photomicrograph of the interface bonding between the AA1050 aluminum and AISI 304 stainless steel with an increase of 100 X. (Alves et al. 2010)

## **Current Technology of Friction Welding**

Thompson is an award-winning manufacturer of a renowned range of rotary and linear friction welding machines and supplier of associated automated production systems. Thompson machines are used by the world's top component makers to join a wide range of parts used in airplanes, cars, construction machines, tractors and trucks as well as for mining and mineral exploration equipment.

Thompson's range of rotary friction welding machines offer many market many market-leading features including a superior welding cylinder and machine base construction, in-weld monitoring system supplied as standard, unique closed loop control of welding pressures and quick tool change facilities. The machines, designed and manufactured to ISO9001: 2000 and ISO14001: 2004 specifications, are available in a selection of models providing forging pressures from 4 tons up to 300 tons. They can be supplied either as a single or double-ended design and with a sliding or fixed head style.

### **2.4 Copper**

Copper and its alloys can be divided into the following three groups: oxygen-free copper, phosphorous deoxidised copper and tough pitch copper. Tough pitch copper contains certain amount of oxygen. In phosphorous deoxidised copper the oxygen level has been significantly reduced by reduction with phosphorous. Oxygen-free copper is usually manufactured to high levels of purity by electrolytic refining. As it contains practically no oxygen that would bind impurities as fairly harmless oxides, the copper content of certified oxygen-free copper is a minimum of 99.99 w-%.

Pure copper is an excellent electrical conductor. Its thermal conductivity is 384W/mK, is about twice that of aluminum and thirty times that of stainless steel; copper is used for components where rapid heat transfer is essential. Copper is non-reactive and does not rust or become brittle in sunlight, make it good in corrosion resistance.

## 2.5 Conventional Lathe Machine

The lathe machine which was used in this study:

Name	: Excel XL-510
Machine Type	: Horizontal
Control	: Manual
Number of Axes	: 2
Cutting Diameter	: 515 mm
Bar / Bore	: 80 mm
Tool Station	: 4
Spindles	: 1
Motor Power	: 7.5 kW
Spindle Speed	: 2000 rpm
Extra Function	: None



Figure 2.6: Excel XL-510 Heavy Duty Lathe Machine

## CHAPTER 3 METHODOLOGY

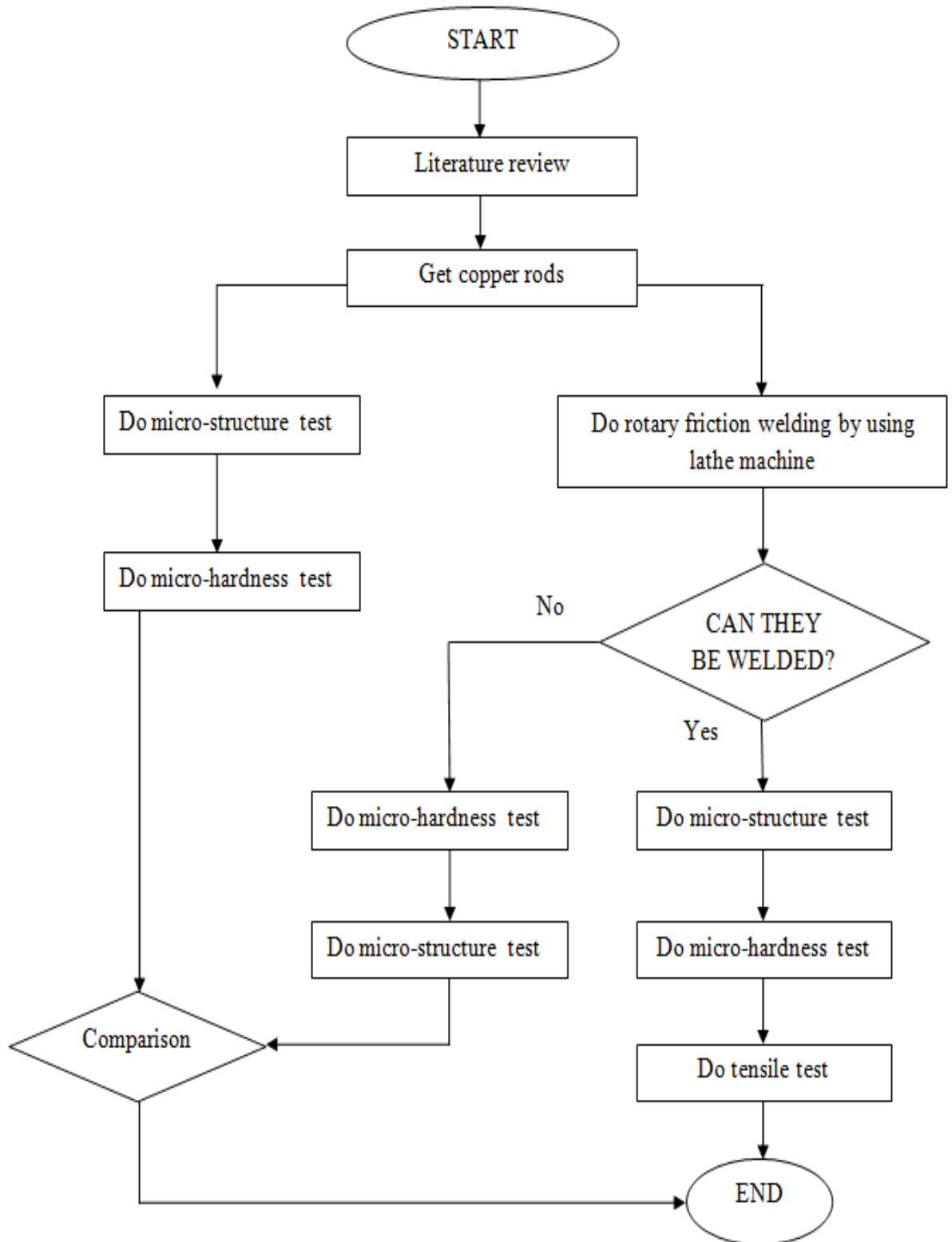
### 3.1 Introduction

By utilizing a conventional lathes machine, axial pressure was applied manually. The only parameter this machine provided is rotational speed, in unit of revolution per minute (rpm).

In order to study the welding temperature, an infrared thermometer was used while the experiment was running. It was used to measure temperature in this experiment because it was safe: it did not have to be in contact with the copper rods, since the rods were heated to high temperature.

Started with a low rotational speed, which was 835 rpm, the experiment was carried out. The speed then was increased; 1320 rpm and 2000 rpm were selected. In these preliminary tests of rotary friction welding, 2000 rpm was the applicable speed because high temperature can be easily achieved for the copper rods. Once the welding process had been carried out, the copper rods were put through the microhardness testing and microstructure testing to study the effects of welding.

### 3.2 Flow Chart



### 3.3 Procedures

#### 3.3.1 Rotary Friction Welding Procedure

1. Copper rods C11000 were bought with dimension of 10mm diameter with 60mm length (Figure 3.1).
2. One copper rod was clamped to the spindle chuck and another one to the stationary chuck (Figure 3.2).
3. These copper rods were brought together as close as possible by moving the stationary chuck holder by rotating tailstock wheel (Figure 3.3). Then, the holder was locked.
4. Rotational speed was adjusted to required speed (Figure 3.4).
5. Clutch was pushed down to spin the flywheel (Figure 3.5). It took a few seconds to rotate at selected speed (Figure 3.6).
6. Force was applied by rotating tailstock wheel to push the stationary copper rod towards rotating copper rod.
7. After the copper rods were heated until red heated, force was keep applied. Clutch was pulled up to stop the spinning of flywheel (Figure 3.7).
8. Temperatures of both copper rods were measured on the surfaces by an infrared thermometer immediately after flywheel stopped (Figure 3.8)
9. Copper rods were removed from the clamping after they were cooled.

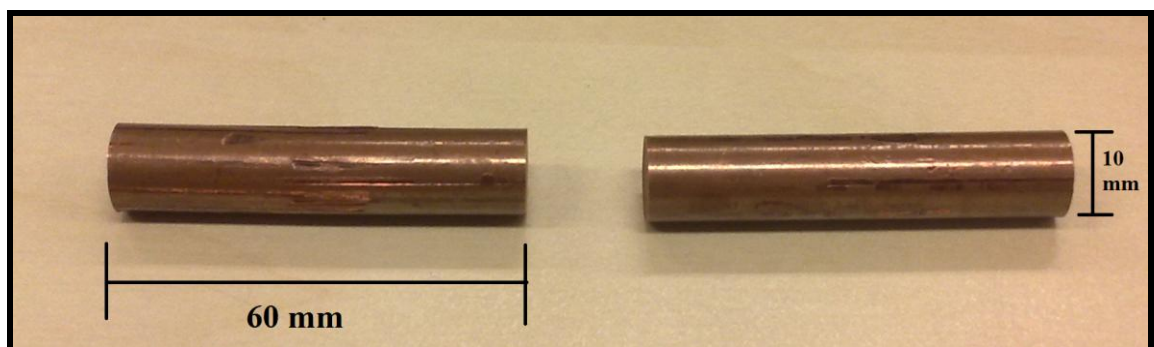


Figure 3.1: Unprocessed copper

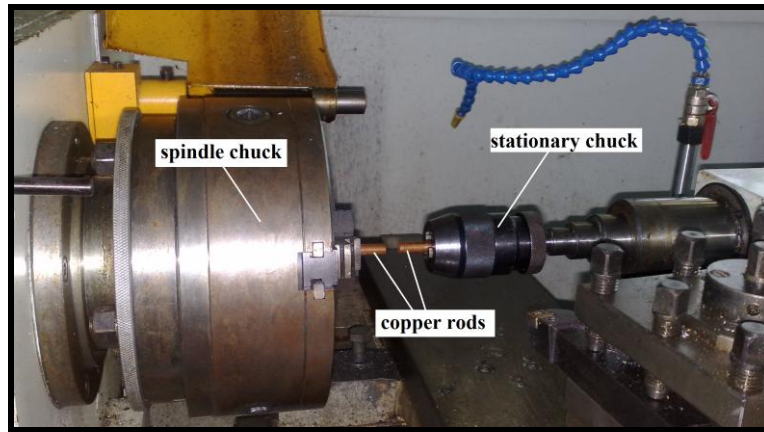


Figure 3.2: Copper rods were clamped to chucks; one to the spindle chuck and another to the stationary chuck.

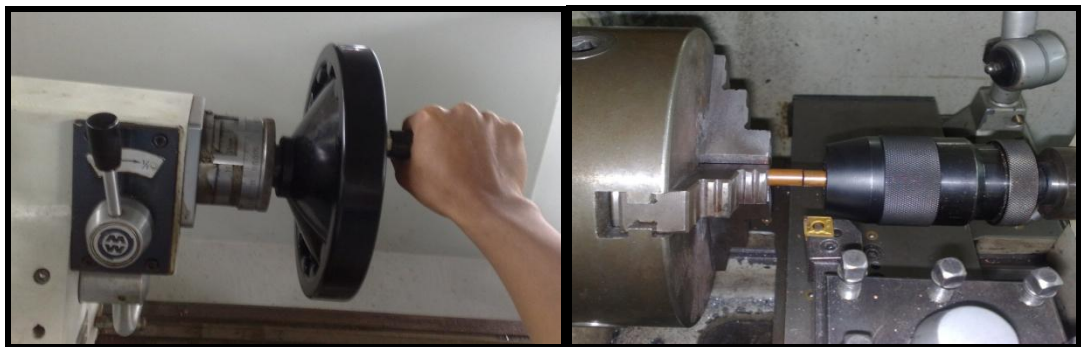


Figure 3.3: Copper rods were brought together as close as possible.



Figure 3.4: Rotational speed was adjusted.



Figure 3.5: Clutch was pushed down.



Figure 3.6: Spindle chuck was rotating.



Figure 3.7: Clutch was pulled up.

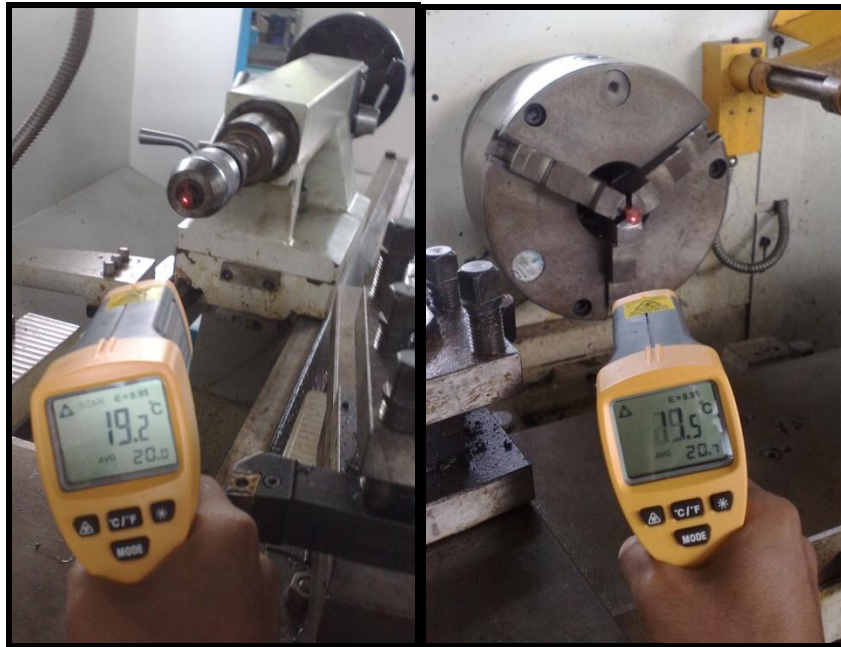


Figure 3.8: Measuring temperatures for both copper rods by using an infrared thermometer.

### 3.3.2 EDM Wire Cutting Procedure

Processed copper rods (Figure 3.9) were cut into semi-circle cross section pieces (Figure 3.11) with length of 10 mm (Figure 3.10) by using an EDM wire cutting machine, Mitsubishi FA10 (Figure 3.12 ).

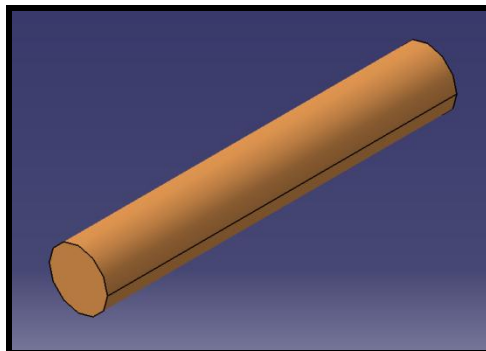


Figure 3.9: 60mm copper rod.

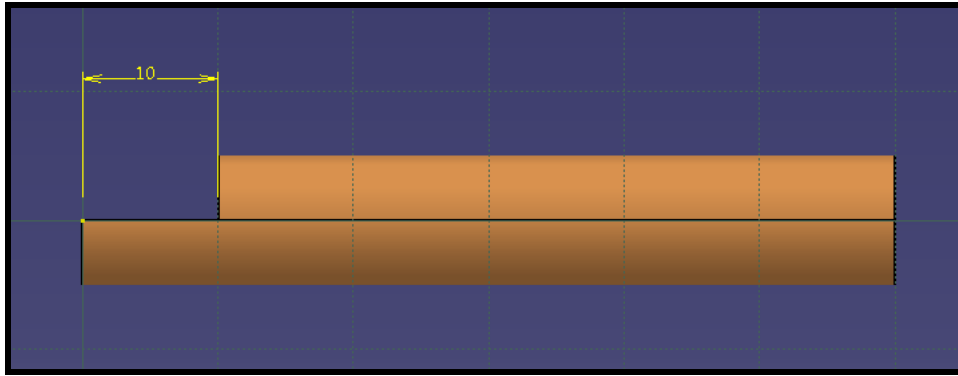


Figure 3.10: Dimension of 10mm to be cut.

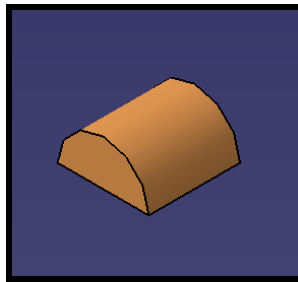


Figure 3.11: Desired size of copper piece prior to mounting for both microstructure and microhardness test.



Figure 3.12: EDM wire cutting machine, Mitsubishi FA10

Figures below are roughly shows the procedure of wire cutting process.

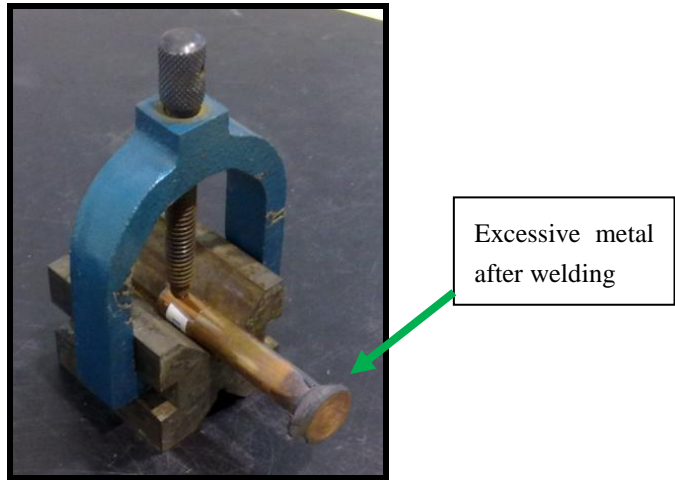


Figure 3.13: Copper rod was clamped.



Figure 3.14: Copper rod was placed to origin position.



Figure 3.15: By using controller, wire was brought close to the copper rod.



Figure 3.16: The cutting tank was filled up with water.



Figure 3.17: Movement of the cutting was programmed by using computer numerical controlled (CNC) drawing plotter.



Figure 3.18: Wire was cutting the copper rods.



Figure 3.19: Copper rods that had been cut.

### 3.3.3 Microstructure Test Procedure (preparation)

In order to identify and evaluate the microstructure of material, it is very important to prepare the test sample carefully and properly. The various steps in sample preparation for microstructural examination as follows:

1. Mounting the section without damage to the test sample
2. Grinding to achieve a flat sample with a minimum amount of damage to the sample surface
3. Polishing the mounted and ground sample
4. Etching in the proper etchant to reveal the microstructural details

#### Mounting

After the copper was cut into the desired size, which was a semi-circle cross-section with 1 cm in length, it was mounted in a plastic or epoxy material to facilitate handling and the grinding and polishing steps. The copper piece was put into a cylinder of compression mounting equipment, which was Buehler Simplimet 1000 Auto Mounting Press (Figure 3.21). In this study, Buehler Phenolic Powder was used as the molding compound (Figure 3.20). One and a half scoop of the powder was poured into the cylinder. With 3 minutes of heating time and 4 minutes of cooling time, the mold was heated and pressurized at 4200psi. Then, the mounted sample was removed from the mold (Figure 3.22).



Figure 3.20: Phenolic powder, manufactured by Buehler.



Figure 3.21: Compression mounting equipment: Simplimet 1000 Auto Mounting Press, manufactured by Buehler.

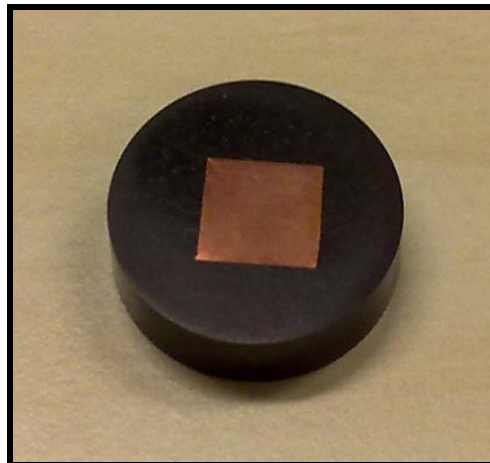


Figure 3.22: Mounted copper.

## Grinding

Grinding follows mounting to remove the surface damaged and to provide a flat surface. Grinding generally involves the use of water lubricated abrasive wheels and the use of a series of progressively finer abrasive grits (Figure 3.25). Grinding papers, Microcut Silicon Carbide Grinding Paper from P400 to P2400 of grits (Figure 3.23) were used on a grinder, Metaserv 2000 manufactured by Buehler (Figure 3.24), to get the mounted copper a flat surface that is nearly free of the disturbed or deformed metal that has been introduced by the mounting process.



Figure 3.23: Grinding papers: Microcut Silicon Carbide Grinding Paper, manufactured by Buehler.



Figure 3.24: Grinder: Metaserv 2000, manufactured by Buehler.



Figure 3.25: Grinding process.

### **Polishing**

The polishing step removes the last thin layer of the deformed metal (Figure 3.29). It leaves a properly prepared sample, ready for examination of the unetched characteristics such as inclusion content or any porosity that may exist. The mounted copper was polished by using a polishing cloth, polishing liquid which was MetaDi Fluid 40-6032 (Figure 3.26) and polishing paste which was MetaDi Diamond Paste (Figure 3.27). The polishing liquid was poured on the polishing cloth. Before polishing started, the polishing paste was put on the surface of mounted copper (Figure 3.28). After polishing, the mounted copper was washed with water followed by ethanol ( $C_2H_5OH$ ).



Figure 3.26: Polishing liquid: MetaDi Fluid 40-6032, manufactured by Buehler.



Figure 3.27: MetaDi Diamond Paste (Grade = 3, Mesh = 8000)



Figure 3.28: Polishing paste on mounted copper.



Figure 3.29: Polishing process.

### **Etching**

The final step was etching to show the microstructure of the test sample. This step reveals features such as grain boundaries, twins and second phase particles not seen in the unetched sample. Aqueous ferric chloride was prepared to be used as etching solution for this copper (Figure 3.30). This etchant then was layered on the surface of mounted copper by using a cotton bud (Figure 3.31). After a few seconds, when the colour of the surface was changed, the mounted copper was washed by using water immediately (Figure 3.32), and then followed by ethanol (Figure 3.33). The surface of mounted copper was dried by using a dryer, Struers Drybox 2 (Figure 3.34). The mounted copper was ready to be put under lens of an optical microscope, Leica DMLM (Figure 3.35).

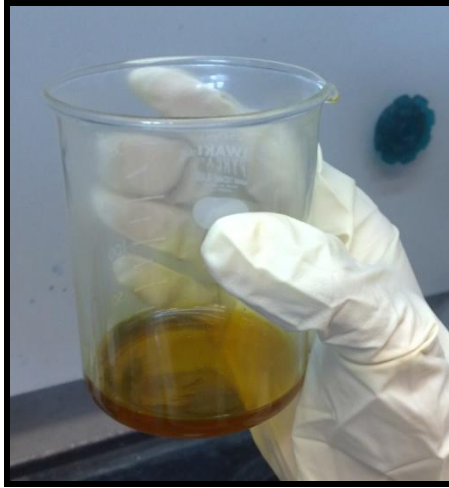


Figure 3.30: Aqueous Ferric Chloride etching solution.

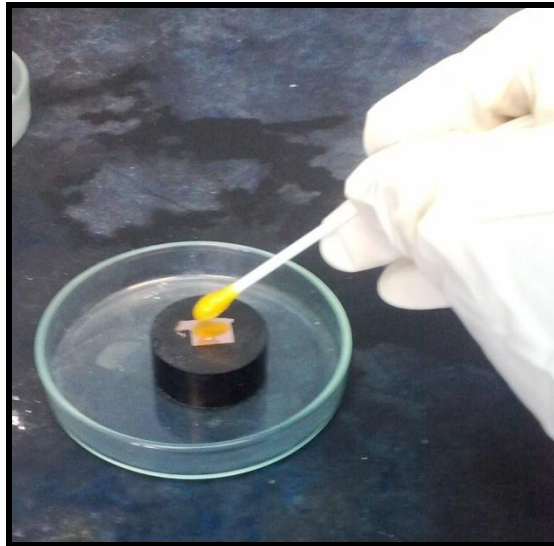


Figure 3.31: Etching solution on mounted copper.



Figure 3.32: Mounted copper was washed by water.



Figure 3.33: Mounted copper was washed by ethanol.

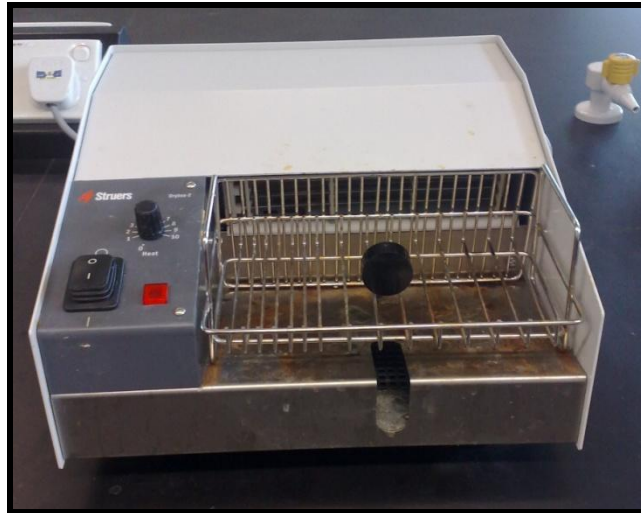


Figure 3.34: Mounted copper was dried by a dryer, Struers Drybox 2, manufactured by Struers.



Figure 3.35: Optical microscope, Leica DMLM

### 3.3.4 Microhardness Test Procedure

In this study, a Vickers Hardness Tester was used to measure the hardness value. It got a diamond pyramid indenter with an included angle of  $136^\circ$ . LECO LM247AT Microhardness Tester was used. The diamond indenter was pressed on to mounted copper to cause a square-based pyramid indentation (Figure 3.36). The load was 200gf and the dwell time was 15 seconds.

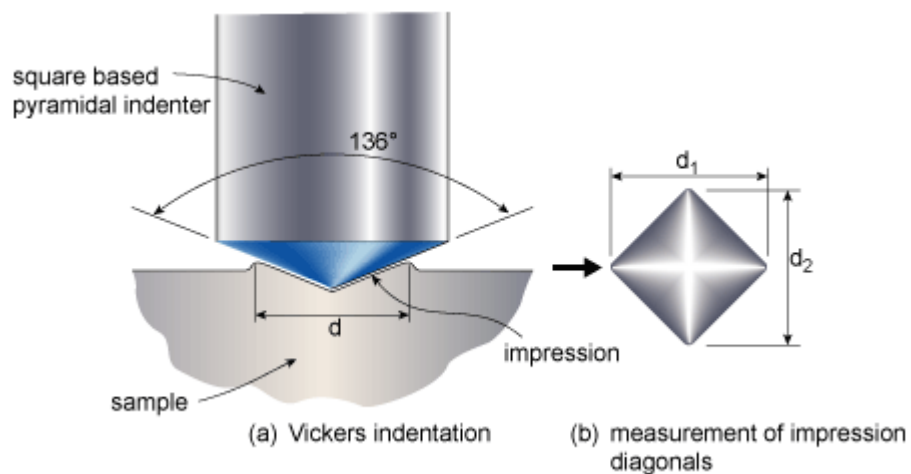


Figure 3.36: Vickers hardness test, (a) Vickers indentation, (b) measurement of impression diagonal

#### Vickers Hardness Method

1. The sample was put under the lens, and was zoomed until microstructure can be seen clearly.
2. Test load was set, which was 200 gf.
3. 'Start' button was pressed. The indenter was pressed into the sample by an accurately controlled test force.
4. The force was maintained for a dwell time that has been set, which was 15 seconds.

5. After the dwell time was completed, the indenter was removed. A square shape appeared on the surface of sample.
6. The size was determined optically by measuring two diagonals of the square indent, which were  $d_1$  and  $d_2$  (Figure 3.36). Hardness value was stated on the screen of the tester (Figure 3.37).

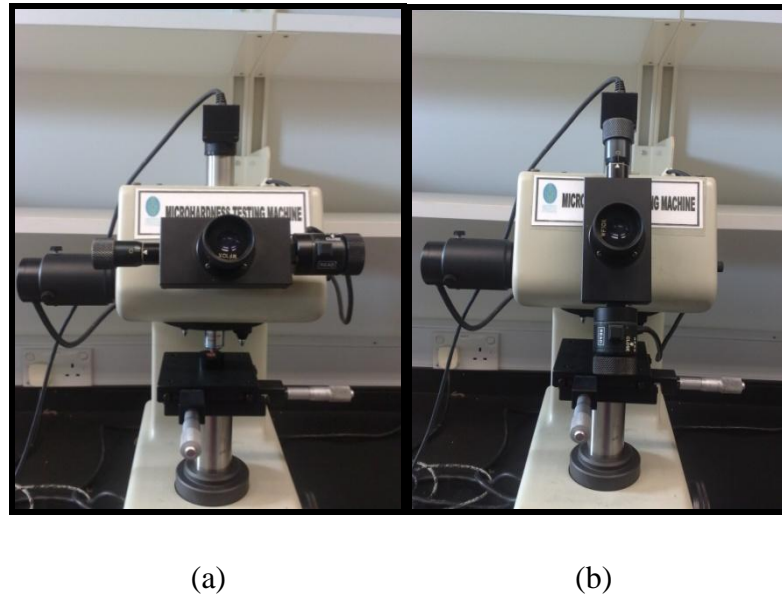


Figure 3.37: LECO LM247AT Microhardness Tester, (a)  $d_1$  measuring eyepiece handle position, (b)  $d_2$  measuring eyepiece handle position



Figure 3.38: Value of hardness was stated on the screen.

### 3.4 Key Milestones (FYP 2 Gantt Chart)

Table 3.1: FYP 2 Gantt Chart

No	Detail / Week	1	2	3	4	5	6	7	8	9	10	11	12	13	14	15
1	Project Work Continues															
2	Submission of Progress Report															
3	Submission of Draft Report															
4	Submission of Softbound															
5	Submission of Technical Paper															
6	Oral Presentation															
7	Submission of Dissertation															

Week 9 to 12

Microhardness and microstructure testing were carried out on these four weeks.

Week 14

Dissertation (softbound) and Oral Presentation were submitted to Supervisor on this week.

Week 15

Final Dissertation (hardbound) and Technical Paper were carried out.

### 3.5 Tools Used

#### 3.5.1 Equipments

The equipments that were used:

- a) Conventional Lathes Machine – Excel XL-510 Heavy Duty Lathe Machine
- b) Vickers Hardness Tester - LECO LM247AT Microhardness Tester
- c) Grinder - Metaserv 2000 (Buehler)
- d) Optical Microscope – Leica DMLM Optical Microscope
- e) EDM Wire Cutting Machine – Mitsubishi FA10
- f) Compression mounting equipment - Simplimet 1000 Auto Mounting Press (Buehler)
- g) Infrared Thermometer - Edison Model IRT537
- h) Dryer - Struers Drybox 2

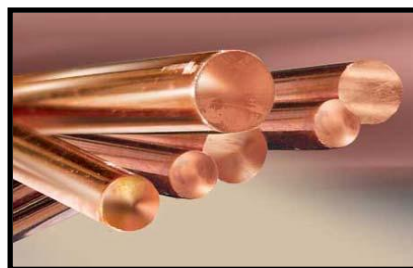
#### 3.5.2 Materials

The materials were pure copper C11000 rod, 10mm diameter with 60mm length.

Table 3.2: Thermal Properties for Copper

Material	Thermal Diffusivity, $\alpha$ (m <sup>2</sup> /s)	Volume Thermal Capacity, $\rho C_s$ (J/m <sup>3</sup> K)	Thermal Conductivity, $k$ (J/m s K)	Melting Point (K)
Copper	$9.6 \times 10^{-5}$	$4.0 \times 10^6$	384.0	1336

Figure 3.39: Copper rods.



## CHAPTER 4 RESULT AND DISCUSSION

### 4.1 Result of Rotary Friction Welding Process

When placed under the optical microscope and microhardness tester, the copper pieces were analyzed and sample data was taken from the copper pieces. The processed copper (Figure 4.2) was compared to unprocessed copper (Figure 4.1).

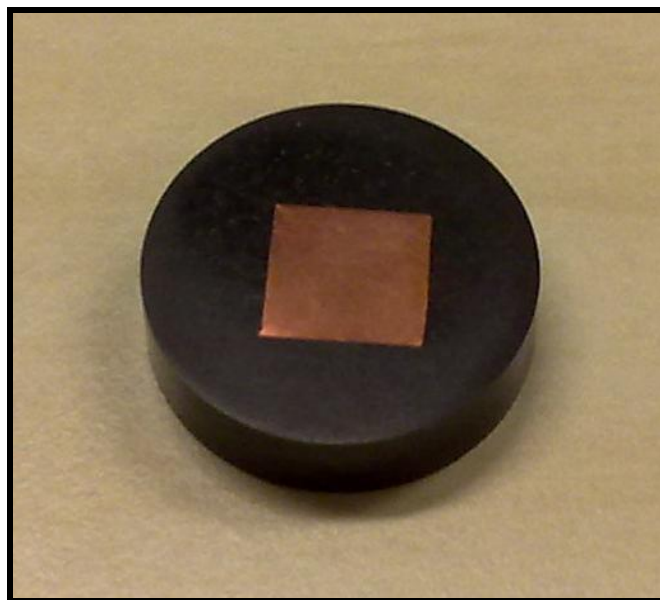


Figure 4.1: Mounted unprocessed copper.



Figure 4.2: Mounted processed copper.

The rotary friction welding result for the processed copper rods:

Table 4.1: Result of friction welding process

No.	Speed (rpm)	Rotated copper rod ( ° C )	Static copper rod ( ° C )	Time (minute)
1	2000	90.6	190.8	12
2	2000	99.7	171.8	15
3	2000	85.9	165.2	10
4	2000	106.7	242.1	5

All of these tests were able to get high temperature until red heat occurred. This was a sign that there is possibility for the conventional lathe machine to perform rotary friction welding of copper rods. Temperatures were low than expected due to uncalibrated equipment. Hence, the infrared thermometer cannot be relied.

## 4.2 Processed Copper Rods

Figure 4.3 and Figure 4.4 below are the result of test number 2 in Table 4.2. Copper rods were 40mm from chuck, the longest in this study. Huge vibration happened; the process of friction welding was quite difficult and took 15 minutes.



Figure 4.3: Bent processed copper.



Figure 4.4: Bent processed copper (top view).

Figure 4.5 and Figure 4.6 below are the result of test number 4 in Table 4.2. Copper rods were 20mm from chuck, the shortest in this study. Least vibration happened; the process of friction welding was easy to be done and took only 5 minutes. This test got the highest temperature, which was 242.1 °C.



Figure 4.5: Shortest processed copper.



Figure 4.6: Shortest processed copper (top view)

### 4.3 Microstructure Test

#### 4.3.1 Microstructure Test Result



Figure 4.7: Microstructure of unprocessed copper – 10x of zooming.

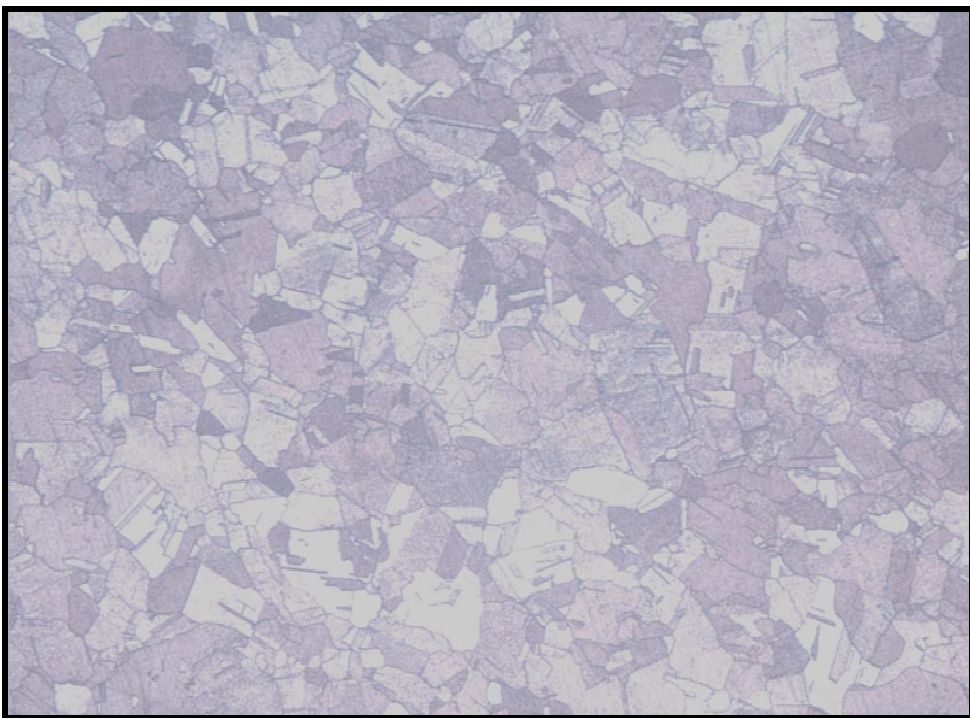


Figure 4.8: Microstructure of processed copper – 10x of zooming.



Figure 4.9: Microstructure of unprocessed copper – 150x of zooming.



Figure 4.10: Microstructure of processed copper – 150x of zooming.

### 4.3.2 Microstructure Test Analysis

Figure 4.7 to Figure 4.10 shows comparison of microstructure features between unprocessed and processed copper, with 10x and 150x of zooming.

In those figures, microstructure of processed copper shows smaller grain size than the unprocessed copper due to the processes of recovery and recrystallization. Recovery occurred at a certain temperature range below recrystallization temperature of the copper, the stresses in the highly deformed regions of the copper piece were relieved. In recrystallization, new equiaxed and strain-free grains were formed, replaced the older grains. Recrystallization decreases the density of dislocations, lowers the strength, and raises the ductility of the metal.

#### 4.4 Microhardness Test

After the microstructure test was done, microhardness of the material was set to be tested. The microhardness testing was carried out by using a Vickers Hardness Tester and the units were in Hardness Vickers (HV). Load was 200gf and the dwell time was 15 seconds.

##### 4.4.1 Microhardness Result of Unprocessed Copper

Table 4.2: Microhardness result of unprocessed copper

No. of test	Hardness Vickers (HV)
1	110.2
2	109.2
3	106.3
4	109.0
5	107.8
Average	<b>108.5</b>

##### 4.4.2 Microhardness Result of Processed Copper

Five points were taken; each point was 1 mm away from each other, as Figure 4.10 below.

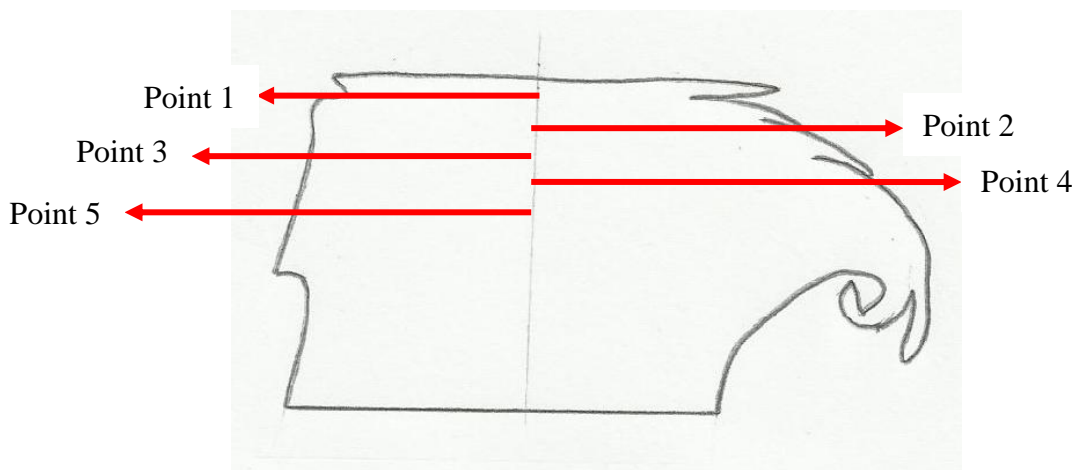


Figure 4.11: Mounted processed copper for indentations.

Table 4.3: Microhardness result of processed copper

Point	Reading 1 (HV)	Reading 2 (HV)	Reading 3 (HV)	Average (HV)
1	71.2	71.0	72.8	71.7
2	70.9	66.7	69.6	69.1
3	71.6	71.2	76.9	73.2
4	76.7	73.0	71.8	73.8
5	69.6	66.3	74.9	70.3
Total average				<b>71.6</b>

#### 4.4.3 Microhardness Test Analysis

Based on the microhardness test that was carried, it can be concluded that the copper rods had gone through an annealing process which reduced the hardness. In the other words, the copper rods became softer.

This processed copper had a hardness value of 71.6 HV. There was a good agreement with Sahin et al. research. In Figure 2.9, Sahin et al got a copper hardness value of 75.0 HV, measured at 3.5mm from weld interface.

## **CHAPTER 5**

### **CONCLUSION AND RECOMMENDATION**

From this study, the experiment was unsuccessful but it showed possibility that rotary friction welding of copper rods can be done since the copper rods were heated until red heat. . Due to the deteriorating machine conditions and the materials, this conventional lathe machine was proven unsuccessfully to perform rotary friction welding of copper rods.

Microstructure test showed that the copper which had gone through annealing process, its grain size become smaller than the unprocessed copper. What happened were recrystallization and recovery of grain. Microhardness test showed hardness value of copper rod reduced after the welding process. Reduced hardness value simply means it become softer.

The biggest problem in this rotary friction welding was the vibration of the work pieces, which were the copper rods. The tailstock quill was too long and the copper rods which were set to a minimum length of 20mm; this was still considered as a long setup.

The temperatures recorded were low and not as expected. All rotary friction welding test showed the red heat; the temperatures should be higher than what stated in the result table. The infrared thermometer that was used in this study must have a faulty; it was an uncalibrated equipment.

As a recommendation, reducing length of work pieces and the length of tailstock quill would be main focus in future study. The target would be reducing the amplitude of vibration by shortening these two parts. A bigger tailstock quill diameter with shorter length should be fabricated or used whereby with these dimension, rotary friction welding process would be more stable and would cause more heat generation. The length of copper rods would be as short as possible in order to reduce the vibration and to increase the stability of the welding process, but they must be not too short because some volume of the rods will turn into flash and chips. In other words, length of copper could be taken into account in future study. If all these modifications are done, rotary friction welding of copper rods probably could be achieved by utilizing the conventional lathes machine.

## REFERENCES

Alves et al. (2010): Eder Paduan Alves, Francisco Piorino Neto, Chen Ying An, Euclides Castorino da Silva, “Experimental Determination of Temperature During Rotary Friction Welding of AA1050 Aluminum with AISI 304 Stainless Steel”, J. Aerosp. Technol. Manag., São José dos Campos, Vol.2, No.3, pp. 301-306, Sep-Dec., 2010.

Avinash et al. (2007): M. Avanish, G.V.K. Chaitanya, Dhananjay Kumar Giri, Sarala Upadhya, and B.K. Muralidhara, “Microstructure and Mechanical Behavior of Rotary Friction Welded Titanium Alloys”, World Academy of Science, Engineering and Technology 35 2007.

Kurt et al. (2011): A. Kurt, I. Uygur, and U. Paylasan, “Effect of Friction Welding Parameters on Mechanical and Microstructural Properties of Dissimilar AISI 1010-ASTM B22 Joints”, Vol. 90, 2011.

Sahin (2001): Mumin Sahin, “Joining of Aluminum and Copper Material with Friction Welding”, Int J Adv Manuf Technol (2010) 49:527-534, 2009.

Sahin et al. (1998): Ahmet Z. Sahin, Bekir S. Yibas, M.Ahmed, J. Nickel, “Analysis of the Friction Welding Process In Relation to the Welding of Copper And Steel Bars”, Journal of Materials Processing Technology 82 (1998) 127-136.

Excel XL-510 Lathe Machine Specification, Retrieved from <http://www.findamachine.com/lathe/EXCEL/XL510>, 14<sup>th</sup> October 2012.

Performing Microstructural Examination, Laboratory Testing Inc., Retrieved from [http://www.labtesting.com/blog/metallography/microstructural\\_examination/](http://www.labtesting.com/blog/metallography/microstructural_examination/), 26<sup>th</sup> December 2012.

Serope Kalpakjian and Steven R. Schmid, “Manufacturing Engineering and Technology”, 6<sup>th</sup> Edition, Pearson, 2010, page 51, 903-904.

Thompson Friction Welding, Retrieved from <http://www.thompson-friction-welding.com/friction-welding-solutions/machines/new-rotary-machines>, 26<sup>th</sup> December 2012.